LA-UR -85-452

CONF-850266--4

Los Alamos National Laboratory is operated by the University of California for the United States Department of Energy under contract W-7405-ENG-36

LA-UR--85-452

DE85 007702

TITLE: HYBRID SIMULATION CODES WITH APPLICATION TO SHOCKS AND UPSTREAM WAVES

AUTHOR(S): D. Winske

SUBMITTED TO Proceedings of the Second International School for Space Simulation, Kapaa, Kauai, Hawaii, Febr. 3-15, 1985

DISCLAIMER

Los Alamos Los Alamos National Laboratory
Los Alamos, New Mexico 87545

FORM NO 836 R4
ST NO 2629 5/81

HYBRID SIMULATION CODES WITH APPLICATION TO SHOCKS AND UPSTREAM WAVES

D. Winske
Los Alamos National Laboratory
Los Alamos, New Mexico, 87545
USA

ABSTRACT. Hybrid codes in which part of the plasma is represented as particles and the rest as a fluid are discussed. In the past few years such codes with particle ions and massless, fluid electrons have been applied to space plasmas, especially to collisionless shocks. All of these simulation codes are one-dimensional and similar in structure, except for how the field equations are solved. We describe in detail the various approaches that are used (resistive Ohm's law, predictor-corrector, Hamiltonian) and compare results from the various codes with examples taken from collisionless shocks and low frequency wave phenomena upstream of shocks.

1. INTRODUCTION

Plasma physics phenomena are characterized by a multitude of length and time scales, primarily due to the different responses of the light electrons and the massive ions to the imposed and self-generated electric and magnetic fields. Typically, one is interested in particular processes which occur on some of these scales and not interested in other processes that occur on shorter or longer time or distance scales. This can be accomplished in numerical simulation by treating the various plasma species in different ways, for example, as discrete particles or as fluids. Hybrid codes are defined as those numerical algorithms in which the various plasma species are treated in a different manner, as distinct from particle codes where all the plasma species are treated as particles or fluid codes where each species (or several species together) is treated as a fluid.

Various types of hybrid codes are of course possible, depending on the problem at hand. One important subclass of hybrid models are those in which there are two (or more) populations of one particular charge species, whose properties on a particular length or time scale are different. For example, consider the interaction of a small, cold electron beam with a hot background electron population (O'Neil

et al., 1971). In this case the unstable waves generated by the presence of the beam strongly affect it, and thus a particle description is needed to correctly model the highly nonlinear dynamics of the beam electrons. On the other hand, the waves do not affect the background population very much. Thus, there is no need to follow the dynamics of each individual background electron; rather, the contribution of the background component can be included simply as a linear dielectric in Poisson's equation. Similar methods can be used when there are several ion populations. For example, in the study of the interaction of an ion ring velocity distribution with a background ion core, Lee and Birdsall (1979) treated the ring ions as discrete particles, with a fluid description for the background ions (and the electrons).

The most common type of hybrid code, however, occurs when the two species involved are the electrons and ions. The simplest kind of hybrid model of this type is to ignore one species entirely. For example, in the study of high frequency electron behavior it is very common to eliminate the ions, except as a charge-neutralizing background. It is also possible to ignore the electrons entirely, as has been done for tearing mode calculations (Dickman et al. (1969) and later work to be cited in the next section). Another useful approximation that is commonly invoked in this type of hybrid model is quasineutrality, which makes use of the fact that the electron (n_e) and ion (n_i) charge densities are nearly equal. If one is interested in scale lengths much larger than the Debye length, the condition $n_e = n_i$ is imposed; for smaller systems, a Boltzmann relation between the electron charge density and the electrostatic potential may be used instead, which gives rise to a nonlinear Poisson equation. (Okuda et al., 1978). Another common approximation involves the electron mass. Depending on the frequency range of interest, the electron mass may be kept (Hewett and Nielson, 1978) or not.

A very common type of hybrid code, and the one of interest throughout the rest of this chapter, treats the electrons as a massless, charge-neutralizing fluid. In recent years this type of model has become widely used in space physics for the study of phenomena at the bow shock (Leroy et al. 1981 and 1982; Leroy and Winske, 1983. Kan and Swift, 1985; Mandt and Kan, 1985), upstream of the bow shock (Winske and Leroy 1984a; Winske et al. 1984 and 1985; Hada and Kennel, 1985), the magnetopause (Swift and Lee, 1983), the magnetotail (Swift, 1983b), and the magnetosphere (Omura et al. 1985; Tanaka and Goodrich, 1985).

While all of the calculations cited here are based on hybrid models with similar properties, there are differences in the way the models are implemented numerically, primarily in how the field equations are solved. Three different techniques, referred to hereafter as the resistive (Ohm's law) method, the predictor-corrector method, and the Hamiltonian method, have been employed. The purpose of this paper is to explain how these various methods work in some detail (Section 2) and then compare results of simulations based on each method (Section 3). The examples chosen are well studied phenomena from the earth's bow shock and the upstream region, and the discussion will emphasize numerics rather than the physics content. A short summary is given in Section 4.

2. DESCRIPTION OF HYBRID CODE MODELS

In this section the numerical schemes used in three hybrid code models are described. In each case particle-in-cell techniques are employed for the ion dynamics, while fluid equations are used for the (massless) electrons. Quasineutrality is assumed and the low frequency (Darwin) approximation is used (Nielson and Lewis, 1976). For the methods described here the one-dimensional nature of the calculation is utilized, but as will be discussed, each of the models has been generalized to two spatial dimensions.

2.1 Resistive Ohm's Law Method

This model was originally devised by Chodura (1975), and further developed by Sgro and Nielson (1976) and Hamasaki *et al.* (1977), for the analysis of laboratory magnetic fusion experiments and more recently for the study of the earth's bow shock by Leroy *et al.* (1981, 1982). The details of the method and references to earlier work are given by Winske and Leroy (1984b). In this method, as in the two to follow, a standard leapfrog scheme is used to advance the particles and fields. The velocities of the particles are known at the half time steps, while positions of the particles and the fields are known at the even time steps (time levels to be denoted by superscripts). Thus, at time step N, we know $\underline{v}^{N-1/2}$, x^N, $\underline{E}^N$, $\underline{B}^N$. To advance the particles, we solve

$$\frac{d\,\underline{v}^N}{dt} = \frac{\underline{v}^{N+1/2} - \underline{v}^{N-1/2}}{\Delta t} = \frac{q}{m}\left(\underline{E}^N + \underline{v}^N \times \underline{B}^N/c\right) \tag{1}$$

implicitly by substituting $\underline{v}^N = (\underline{v}^{N+1/2} + \underline{v}^{N-1/2})/2$ and solving to obtain

$$\underline{v}^{N+1/2} = f\,\underline{v}^{N-1/2} + \frac{\Delta tq}{m}\left(\underline{E}^N + g\underline{B}^N + \underline{v}^N \times \underline{B}^N/c\right) \tag{2}$$

where

$$\underline{v}^N = \underline{v}^{N-1/2} + \frac{\Delta tq}{2m}\underline{E}^N$$

$$f = 1 - \frac{1}{2}\left(\frac{\Delta tq}{mc}\right)^2 \underline{B}^N \cdot \underline{B}^N \tag{3}$$

$$g = \frac{\Delta tq}{mc^2}\left(\underline{v}^{N-1/2} \cdot \underline{B}^N\right)$$

and then

$$x^{N+1} = x^N + \Delta t v_x^{N+1/2} \tag{4}$$

We then solve Ampere's law

$$\nabla^2 \underline{A}_T^{N+1} = -\frac{4\pi}{c}\underline{J}_T^{N+1} \tag{5}$$

for the transverse components (y or z). The ion part of the current comes directly from collecting the ion moments, where we advance (but do not save) the particles one additional half time step

$$\underline{v}^{N+1} = \underline{v}^{N+1/2} + \frac{\Delta tq}{2m}\left(E^N + \underline{v}^{N+1/2} \times \underline{B}^N/c\right) \tag{6}$$

where $\underline{E}^N$ and $\underline{B}^N$ are evaluated at x^{N+1}, to obtain the ion density n_i^{N+1} and velocities $\underline{V}_i^{N+1}$. Quasineutrality (in 1-D) then gives $n_e = n_i = n$ and $V_{ex} = V_{ix} = V_x$.

The electron part of the current comes from the electron momentum equation with a resistive term (i.e. Ohm's law)

$$m_e \frac{d\underline{V}_e}{dt} = 0 = -qn_e\left(\underline{E} + \frac{\underline{V}_e \times \underline{B}}{c}\right) - \hat{x}\,\frac{\partial}{\partial x} n_e T_e + qn_e \underline{\eta}\cdot\underline{J} \tag{7}$$

After solving for $\underline{A}_T^{N+1}$ (described shortly), we obtain in the usual way

$$\underline{B}_T = \underline{\nabla} \times \underline{A}_T \quad (B_x = \text{constant})$$
$$\underline{E}_T = \frac{-1}{c}\frac{\partial \underline{A}_T}{\partial t} \tag{8}$$

Then solving an energy equation for T_e,

$$\frac{3}{2}\frac{\partial}{\partial t} nT_e + \frac{\partial}{\partial x}\left(\frac{3}{2} nT_e V_{ex}\right) + nT_e \frac{\partial V_{ex}}{\partial x} = \eta J^2 \tag{9}$$

we can obtain the last field component, E_x, from the x component of (7)

$$E_x = \frac{-1}{c}(\underline{V}_e \times \underline{B})_x - \frac{1}{nq}\frac{\partial nT_e}{\partial x} \tag{10}$$

The method used to solve (5) for $\underline{A}_T$ is slightly different from that presented in Winske and Leroy (1984b) and works better for oblique shocks. We assume the resistivity tensor to be diagonal (i.e. $\eta_{\parallel} = \eta_{\perp} = \eta$), which has been shown to correctly model turbulent systems, such as the z-pinch, very well (Sgro and Nielson, 1976). We solve

$$\underline{J}_T = \eta^{-1}(\underline{E} + \underline{V}_e \times \underline{B}/c)_T = qn(V_i - V_e)_T \tag{11}$$

for $\underline{V}_{eT}$, and substitute into (5), obtaining

$$\frac{-c}{4\pi}\frac{\partial^2 A_y}{\partial x^2} = \frac{F_y + \delta F_z}{1 + \delta^2}$$
$$\frac{-c}{4\pi}\frac{\partial^2 A_z}{\partial x^2} = \frac{F_z - \delta F_y}{1 + \delta^2} \tag{12}$$

where

$$F_y = qn\left(V_{iy} - \frac{cE_z}{B_x} - \frac{V_x B_y}{B_x}\right)$$
$$F_z = qn\left(V_{iz} + \frac{cE_y}{B_x} - \frac{V_x B_z}{B_x}\right) \tag{13}$$

$$\delta = \left(\frac{n}{n_o}\right)\left(\frac{\omega_{io}^2 \eta}{4\pi}\right)\left(\frac{mc}{qB_x}\right)$$

and n_o=reference density, $\omega_{io}=(4\pi n_o q^2/m)^{1/2}$, and all quantities are at time level N+1. Using (8) to express $\underline{E}_T$ and $\underline{B}_T$ in terms of $\underline{A}_T$, (12) can be written in finite difference form and solved, as described in Winske and Leroy (1984b).

In addition to the references cited in Winske and Leroy (1984b), calculations based on this method have been done to study oblique shocks (Leroy and Winske, 1983), the electromagnetic ion beam instability (Winske and Leroy, 1984a), the interaction of heavy ions with the solar wind (Winske *et al.* 1984 and 1985) and the steepening of slow waves (Hada and Kennel, 1985). The method has been extended to two dimensions (Hewett, 1980) and has been applied to the study of magnetic reconnection in laboratory experiments (Hewett, 1984).

2.2 Predictor-Corrector Method

A second method used for hybrid code calculations employs the predictor-corrector technique. The method is described by Byers *et al.* (1978) and has been implemented in a one-dimensional code by Tanaka and Goodrich (1985) and Omura *et al.* (1985) in the study of heating of heavy ions by ion cyclotion instabilities. The method has been extended to two dimensions by Harned (1982) and used in the study of rotational instabilities in laboratory field-reversed configurations (Harned, 1983).

We will describe the method in its simplest form, where the electron temperature is kept constant. Again, we assume at time step N the $\underline{v}^{N-1/2}$, x^N, $\underline{E}^N$ and $\underline{B}^N$ are known. In this case the advance of one time step involves two steps, a predictor step and a corrector step, each of which involves going through the particle table.

In the first step, $\underline{v}^{N+1/2}$ and x^{N+1} are obtained as in the previous case using (1) - (4). In the process, however, we first advance the particles to $x^{N+1/2}=x^N+\Delta t v_x^{N+1/2}/2$ to collect the ion moments, $\underline{J}_i^{N+1/2}$ and $n_i^{N+1/2}$. We then compute the predictor fields (denoted by subscript p) using Faraday's law and (7):

$$\underline{B}^{N+1/2} = \underline{B}^N - \frac{c\Delta t}{2}(\nabla \times \underline{E}^N)$$

$$\underline{E}^{N+1/2} = \frac{1}{qn_i^{N+1/2}}\left\{\left(\frac{\nabla \times \underline{B}^{N+1/2}}{4\pi} - \frac{\underline{J}_i^{N+1/2}}{c}\right) \times \underline{B}^{N+1/2} - T_e \nabla n_i^{N+1/2}\right\} \tag{14}$$

to obtain

$$\underline{E}_p^{N+1} = -\underline{E}^N + 2\underline{E}^{N+1/2}$$

$$\underline{B}_p^{N+1} = \underline{B}^{N+1/2} - \frac{c\Delta t}{2}(\nabla \times \underline{E}_p^{N+1}) \tag{15}$$

We then go thru the particles again, using the predictor fields, to calculate $\underline{v}_p^{N+3/2}$ and $\underline{x}_p^{N+3/2}$, again using (1) - (4), in order to collect $\underline{J}_{i,p}^{N+3/2}$ and $n_{i,p}^{N+3/2}$. Then, we calculate $\underline{B}_p^{N+3/2}$ and $\underline{E}_p^{N+3/2}$ using (14) with predictor fields $\underline{E}_p^{N+1}$, $\underline{B}_p^{N+1}$ and ion moments to obtain the new fields

$$\underline{E}^{N+1} = \frac{1}{2}\left(\underline{E}^{N+1/2} + \underline{E}_p^{N+3/2}\right)$$
$$\underline{B}^{N+1} = \underline{B}^{N+1/2} - \frac{c\Delta t}{2}\left(\nabla \times \underline{E}^{N+1}\right) \qquad (16)$$

Having now advanced the fields, we are thus ready to start the entire sequence again.

2.3 Hamiltonian Method

This method employs the canonical momenta of the particles $\underline{P}$ in place of the velocities. A description of the method is given, for example, by Morse and Nielson (1971), and a comparison between the Hamiltonian and Lagragian methods is discussed by Nielson and Lewis (1976). The Hamiltonian method has been used by Swift and Lee (1983) to study the rotational discontinuity at the magnetopause, Swift (1983b) to examine magnetic slow shocks, Kan and Swift (1983) and Mandt and Kan (1985) to simulate nearly parallel shocks. The method has been generalized to two spatial dimensions in the limited sense of either completely ignoring the electrons (Dickman et al.,1969; Ambrosiano et al.; 1983; Teresawa, 1981) for the study of tearing modes and ion fusion physics (Friedman et al., 1977; Mankofsky et al., 1981; Mankofsky and Sudan, 1984) or in restricting the types of perturbations allowed (Swift, 1983a).

In this case, at time step N, the canonical momenta of the particles

$$\underline{P}_T = m\underline{v}_T + q\underline{A}_T/c \qquad (17)$$

are known at the half time step N-1/2. The particle equation of motion is

$$\frac{d\underline{P}_T}{dt} = \frac{q}{c}\left(\underline{v}_T \times B_x \hat{x}\right) \qquad (18)$$

Note that in the case B_x=0 the method can be very attractive since $\underline{P}_T$ is a conserved quantity. Using (17), (18) can be written as

$$\frac{d\underline{P}_T}{dt} = \frac{qB_x}{mc}\left(\underline{P}_T - \frac{q\underline{A}_T}{c}\right) \times \hat{x} \qquad (19)$$

Another nice feature is that using a complex representation ($P = P_y + iP_z$, $A = A_y + iA_z$, $\Omega = qB_x/mc$) the equations of motion can be written compactly as

$$\frac{dP^N}{dt} = -i\Omega\left(P^N - \frac{qA^N}{c}\right) \qquad (20)$$

or

$$e^{-i\Omega t}\frac{d}{dt}P^N e^{i\Omega t} = \frac{i\Omega q A^N}{c} \qquad (21)$$

Thus, in difference form (Swift and Lee, 1983)

$$P^{N+1/2} = P^{N-1/2}e^{-i\Omega\Delta t} + \frac{i\Delta t\Omega q}{c} A^N e^{-i\Omega\Delta t/2} \qquad (22)$$

Then

$$\underline{v}_T^N = \frac{1}{2m}(\underline{P}_T^{N+1/2} + \underline{P}_T^{N-1/2}) - \frac{q\underline{A}_T^N}{mc} \qquad (23)$$

is known and v_x can be advanced

$$v_x^{N+1/2} = v_x^{N-1/2} + \frac{q\Delta t}{m}(E_x^N + \underline{v}_T^N \times \underline{B}_T^N/c) \qquad (24)$$

as can the particle positions, x^{N+1}, using (4). (I have used v_x here for simplicity. It is possible to write $P_x = mv_x$ (A_x=0, since $\underline{\nabla}\cdot\underline{A} = 0$) and use P's throughout.)

Again, we need to solve Ampere's law (5). There are several different ways to difference the equations. One method is to use (22) to advance $P_T^{N+1/2}$ to $P_T^{N+3/2}$ and express it in terms of $P_T^{N+1/2}$ and A_T^{N+1}. Another (Swift and Lee, 1983) is to solve $\nabla^2\underline{A}_T^{N+1/2} = -4\pi\underline{J}_T^{N+1/2}/c$, expressing $\underline{A}_T^{N+1/2}$ as an average between $\underline{A}_T^N$ and $\underline{A}_T^{N+1}$. In either case the resulting equation is implicit in that it involves $\underline{A}_T^{N+1}$ on the right hand side. This adds a slight complication, known as double area weighting, in gathering the moments, as described by Forslund et al. (1972), Forslund (1974) and Mankofsky et al. (1981). Once $\underline{A}_T^{N+1}$ is known, $\underline{E}$ and $\underline{B}$ can be obtained using (8). An equation for T_e, such as (9), can be solved (Kan and Swift (1983) use an equation of state instead), and then E_x can be obtained as before, from (10).

Finally, it should be noted that there is an extra complication if there is an external B_y or B_z in the system. A constant B_z can be added in through an additional term $A_y = B_z x$. This contribution to P_y of the particles must be added or subtracted if the boundary conditions are such that particles exiting at one end of the system reenter at the other end.

3. NUMERICAL COMPARISON OF THE MODELS

In this section we compare results of simulations based on the three hybrid models discussed previously for two test problems. The first is an electromagnetic ion beam instability, the second is a quasiperpendicular collisionless shock. Both problems have been well studied, and the reader is referred to the literature for details.

The first problem involves the ion beam instability, which is thought to be the mechanism which produces low frequency hydromagnetic waves and diffuse ion populations upstream of the earth's bow shock (e.g., see Gary et al. (1981) and Winske and Leroy (1984a)). The instability results from the interaction of a weak

beam of ions backstreaming from the shock and the incident solar wind. The situation to be simulated consists of an ion beam drifting relative to an ambient plasma along a uniform magnetic field B_o. The parameters are chosen to match those in Winske and Leroy (1984a) for the resonant instability: the beam is weak, 1.5% of the total ion density, with a drift speed of 10 V_A relative to the background ions. Both ion components have $\beta=8\pi nT/B_o^2=1.0$, with a cold ($\beta_e=0.01$) current-neutralizing electron background. The instability leads to the generation of low frequency waves of well defined wavelength that scatter the beam. In the nonlinear regime these regular waves break up into very nonlinear waveforms, producing a diffuse ion distribution in the process.

In Figure 1 we compare results of three simulation. The top panels correspond to the resistive code with $\eta=0$; the middle panels are from the predictor-corrector code; the bottom panels are from a code based on the Hamiltonian method. In each case we have used 10,000 particles (half to represent the beam, half for the background ions) on a grid of 256 cells with cell size $\Delta x=c/\omega_i$. In each case we use the same random numbers to initialize the particle velocities. The left side of the figure shows one component of the magnetic field, B_z, normalized in terms of the ambient field B_o at about the time when the waves have achieved their largest amptitude, $\Omega_i t=38.4$ ($\Omega_i=eB_o/m_ic$). The results from the three cases are very similar, differing only in the amount of low amptitude, short wavelength noise that is superimposed on the dominant structures. The right side of the figure shows the time histories of the fluctuating magnetic field energy density, $W_b=\int dx B_T^2/\int dx B_o^2$. Again, the overall results in each case agree very well. The peak field energy density achieved is slightly (~3%) larger in the predictor-corrector case, which may be a reflection of the better energy conservation in the predictor-corrector code ($\Delta E/E_o$~0.03%), compared with the resistive code ($\Delta E/E_o$~1.2%) and the Hamiltonian code ($\Delta E/E_o$~5.4%). The poorer energy conservation in the Hamiltonian code suggests that the differencing scheme used here for the test problem could be improved and should not be taken as an indication that this method is inherently inferior.

The second test problem involves a quasiperpendicular collisionless shock. Again, in this case the physics has been investigated in detail (Leroy et al, 1981 and 1982; Leroy and Winske, 1983; Forslund et al., 1984). The simulation is initialized with uniform upstream and downstream states related by Rankine-Hugoniot conditions and then is allowed to evolve in time. The parameters chosen for the test case are upstream Mach number $M_A=V_1/V_A=8$, upstream shock normal angle $\theta_{Bn}=60°$, and upstream $\beta_e=\beta_i=0.5$. Again, we show (Figure 2) the results of three simulations: top panels correspond to the resistive code with resistive length $L_R=(n\omega_i/4\pi)(c/V_1)(c/\omega_i)$ equal to the cell size $\Delta x=0.3\ c/\omega_i$, middle panels correspond to the results of the resistive code with $L_R=0.01\Delta x$, and bottom panels correspond to the resistance-free predictor-corrector code. In each case 10,000 particles on a grid of 200 cells with a time step $\Omega_i\Delta t=0.0125$ (where the upstream magnetic field B, is used to compute Ω_i).

The left side of Figure 2 shows one component of the transverse magnetic field B_z at $\Omega_i t=12.5$. The upstream magnetic field is to the left in each picture; the shock occurs in the center where the magnetic field rises rapidly. The peak value of the magnetic field component B_z is somewhat larger than the downstream value B_{z2} (computed from the Rankine-Hugoniot relations), which is held fixed at the right hand boundary. This peak value, referred to as the overshoot, is followed by an undershoot and then several more oscillations. The middle panel shows the same snapshot of the magnetic field in the run where the resistivity is lowered. The same overall stucture is observed, except that the overshoot is larger and the oscillations behind the overshoot are somewhat less regular. In addition, there are small oscillations on the magnetic field in the upstream region and the sharp rise of the magnetic field is better resolved, consisting of a precursory smaller increase (called the foot) and a very steep ramp. The field profile obtained with the predictor-corrector code (bottom panel) shows the same general features as in the second case, except that the oscillations behind the shock are somewhat larger in amplitude and have a shorter wavelength.

The right hand panels of Figure 2 show the time histories of the magnetic overshoot for the three runs. In the case with the larger resistivity, the overshoot has a nearly constant value. For small resistivity, the overshoot oscillates in time and the average value is about 20% larger. The resistance-free predictor-corrector code gives a slightly larger average overshoot with larger, more frequent oscillations.

We conclude from these results that the three shock simulations give overall similar results, but the effect of resistivity is to damp out some of the oscillations. This naturally leads to the question of how much resistivity (if any) should be included. It should be kept in mind that the resistivity is added in to compensate for the fact that the simulations are one-dimensional and therefore do not include microinstabilities due to the cross-field current that are seen, for example, in 2-D particle simulations of shocks (Forslund et al., 1984). In the present simulations, as in Leroy et al. (1982), the resistivity is taken as a constant, although more realistic forms for the resistivity, either based on phenomenological expressions (Chodura, 1975) or microphysics (Hamasaki et al., 1977) are possible. In this regard, one has to be guided by space observations or laboratory data (which indeed show rather steady structures) to infer the proper amount of resistivity that should be used.

As a final note, the question of resistivity becomes increasingly complex as the Mach number is raised. Quest (1985) has recently carried out resistive hybrid simulations of perpendicular shocks with Mach numbers greater than 20. He finds that a shock which is fairly steady in time can be produced with resistivity such that $L_R=\Delta x$, but that with weaker resistivity the magnitude of the oscillations of the overshoot is comparable to its average value. In this case the shock steepens to a very narrow ($\sim\Delta x$) width, then collapses. Because the amount of resistivity that would be needed to maintain the shock steady is unphysically large at high Mach numbers, it is suggested that very high Mach number shocks indeed are oscillatory in character (Quest, 1985).

4. SUMMARY

We have described hybrid codes in which the various plasma species are given different representations. Specializing to the important case where the ions are treated as particles and the electrons are a massless, charge-neutralizing fluid, we have discussed in some detail three ways for solving the field equations, referred to here as the resistive, predictor-corrector, and Hamiltonian methods. Using simulation codes based on each of these techniques, we have compared results for two problems of current interest in space physics: low frequency waves driven by an ion beam and quasiperpendicular collisionless shocks. For the ion beam problem all three methods give essentially the same results, with the predictor-corrector method giving better overall energy conservation. In the case of the quasiperpendicular shock, the effect of the resistivity on producing time steady solutions has been emphasized. While the use of these codes in one spatial dimension has been stressed throughout this article, all three methods discussed work in two dimensions, and will undoubtedly become widely applied in space physics, as they have already in magnetic fusion problems.

ACKNOWLEDGEMENTS. This work was supported by the NASA Solar-Terrestrial Theory Program and the Department of Energy.

REFERENCES

Ambrosiano, J.J., L.C. Lee, and D.W. Swift, 'Simulation of the ion tearing instability in the presence of a background plasma', J. Geophys. Res., 88, 7860, 1983.

Byers, J.A., B.I. Cohen, W.C. Condit, and J.D. Hanson, 'Hybrid simulations of quasineutral phenomena in magnetized plasma', J. Comp. Phys., 27, 363, 1978.

Chodura, R., 'A hybrid particle-fluid model of ion heating in high Mach number shock waves', Nucl. Fusion, 15, 55, 1975.

Dickman, D.O., R.L. Morse, and C.W. Nielson, 'Numerical simulation of axisymmetric collisionless finite-beta plasma', Phys. Fluids, 12, 1708, 1969.

Forslund, D.W., 'Plasma simulation techniques and their use', Los Alamos Scientific Laboratory Report, LA-UR 74-1333, 1974.

Forslund, D.W., E.L. Lindman, R.W. Mitchell, and R.L. Morse, 'EMI a general purpose one-dimensional electromagnetic particle simulation code', Los Alamos Scientific Laboratory Report, LA-DC 72-721, 1972.

Forslund, D.W., K.B. Quest, J.U. Brackbill, and K. Lee, 'Collisionless dissipation in quasiperpendicular shocks', J. Geophys. Res., 89, 2142, 1984.

Friedman, A., R.L. Ferch, R.N. Sudan, and A.T. Drobot, 'Numerical simulation of strong proton rings', Plasma Phys., 19, 1101, 1977.

Gary, S.P., J.T. Gosling, and D.W. Forslund, 'The electromagnetic ion beam instability upstream of the earth's bow shock', J. Geophys. Res., 86, 6691, 1981.

Hada, T., and C.F. Kennel, 'Nonlinear evolution of slow waves in the solar wind', J.Geophys. Res., 90, in press, 1985.

Hamasaki, S., N.A. Krall, E.E. Wagner, and R.N. Byrne, 'Effect of turbulence on theta pinch modeling by hybrid numerical models', Phys. Fluids, 20, 65, 1977.

Harned, D.S., 'Quasineutral hybrid simulation of macroscopic plasma phenomena', J. Comp. Phys., 47, 452, 1982.

Harned, D.S., 'Rotational instabilities in the field reversed configuration: results of hybrid simulations', Phys. Fluids, 26, 1320, 1983.

Hewett, D.W., 'A Global method for solving the electron-field equations in a zero-inertia-electron hybrid plasma simulation code', J. Comp. Phys., 38, 378, 1980.

Hewett, D.W., 'Spontaneous development of toroidal magnetic field during formation of field reversed theta pinch', Nucl. Fusion, 24, 349, 1984.

Hewett, D.W., and C.W. Nielson, ' A multidimensional quasineutral plasma simulation model', J. Comp. Phys., 29, 219, 1978.

Kan, J.R., and D.W. Swift, 'Structure of the quasiparallel bow shock: results of numerical simulations', J. Geophys. Res., 88, 6919, 1983.

Lee, J.K., and C.K. Birdsall, 'Velocity space ring plasma instability, magnetized, part II: simulations', Phys. Fluids, 22, 1315, 1979.

Leroy, M.M., C.C. Goodrich, D. Winske, C.S. Wu, and K. Papadopoulos, 'Simulation of a perpendicular bow shock', Geophys. Res. Lett., 8, 1269, 1981.

Leroy, M.M., D. Winske, C.C. Goodrich, C.S. Wu, and K. Papadopoulos, 'The structure of perpendicular bow shocks', J. Geophys. Res., 87, 5081, 1982.

Leroy, M.M., and D. Winske, 'Backstreaming ions from oblique earth bow shocks', Ann. Geophysicae, 1, 527, 1983.

Mandt, M.E., and J.R. Kan, 'Effects of electron pressure in quasiparallel collisionless shocks', J. Geophys. Res., 90, in press, 1985.

Mankofsky, A., A. Friedman, and R.N. Sudan, 'Numerical simulation of injection and resistive trapping of ion rings', Plasma Phys., 23, 521, 1981.

Mankofsky, A., and R.N. Sudan, 'Numerical simulation of ion beam propagation in Z pinch plasma channels', Nucl. Fusion, 24, 827, 1984.

Morse, R.L., and C.W. Nielson, 'Numerical simulation of the Weibel instability in one and two dimensions', Phys. Fluids, 14, 830, 1971.

Nielson, C.W., and H.R. Lewis, 'Particle code models in the nonradiative limit', in Methods of Computational Physics. Vol. 16, edited by J. Killeen, B. Alder, S. Fernbach, and M. Rotenberg, p. 367, Academic Press, New York, 1976.

Okuda, H., J.M. Dawson, A.T. Lin, and C.C. Lin, 'Quasineutral particle simulation model with application to ion wave propagation', Phys. Fluids, 21, 476, 1978.

Omura, Y., M. Ashour-Abdalla, K. Quest, and R. Gendrin, 'Heating of thermal helium in the equatorial magnetosphere: a simulation study', J. Geophys. Res., 90, in press, 1985.

O'Neil, T.M., J.H. Winfrey, and J.H. Malmberg, 'Nonlinear interaction of a small cold beam and a plasma', Phys Fluids, 14, 1204, 1971.

Quest, K.B., 'Simulations of high Mach number collsionless shocks', Phys. Rev. Lett., submitted. 1985.

Sgro, A.G., and C.W. Nielson, 'Hybrid model studies of ion dynamics and magnetic field diffusion during pinch implosions', Phys. Fluids, 19, 126, 1976.

Swift, D.W., 'A two-dimensional simulation of the interaction of the plasma sheet with the lobes of the earth's magnetotail', J.Geophys. Res., 88, 125, 1983a.

Swift, D.W., 'On the structure of the magnetic slow switch-off shock', J.Geophys. Res., 88, 5685, 1983b.

Swift, D.W., and L.C. Lee, 'Rotational discontinuities and the structure of the magnetopause', J.Geophys. Res., 88, 111, 1983.

Tanaka, M., and C.C. Goodrich, 'Simulation study of heavy ion heating by electromagnetic ion cyclotion waves induced by proton temperature anisotropy', J. Geophys. Res., 90, in press, 1985.

Teresawa, T., 'Numerical study of explosive tearing mode instability in one component plasmas', J. Geophys. Res., 86, 9007, 1981.

Winske, D., and M.M. Leroy, 'Diffuse ions produced by electromagnetic ion beam instabilities', J. Geophys. Res., 89, 2673, 1984a.

Winske, D., and M.M. Leroy, 'Hybrid simulation techniques applied to the earth's bow shock', in Computer Simulations of Space Plasmas, edited by H. Matsumoto and T. Sato, D. Reidel/Terra, Hingham, Mass., 1984b.

Winske, D., C.S. Wu, Y.Y. Li, and G.C. Zhou, 'Collective capture of released lithium ions in the solar wind', J. Geophys. Res., 89, 7327, 1984.

Winske, D., C.S. Wu, Y.Y. Li, Z.Z. Mou, and S.Y. Guo, 'Coupling of newborn ions to the solar wind by electromagnetic instabilities and their interaction with the bow shock', J. Geophys. Res., 90, in press, 1985.

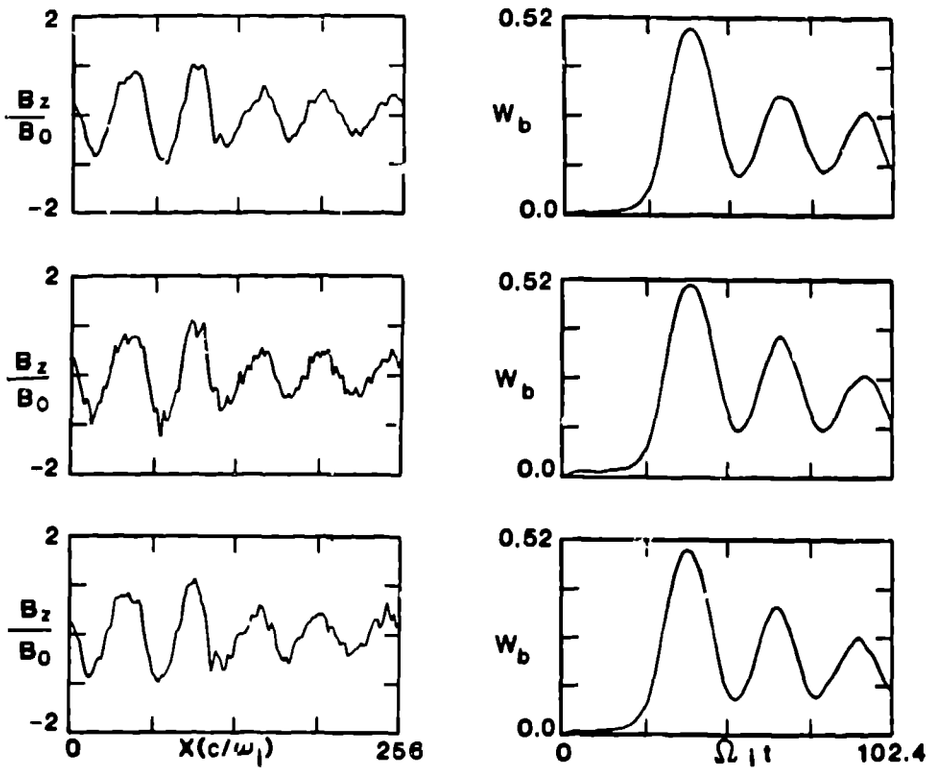

Figure 1. Results of three different hybrid simulations of the electromagnetic ion beam instability (top: resistive model; middle: predictor-corrector model; bottom: Hamiltonian model) showing: (left) one component of the fluctuating magnetic field at $\Omega_i t = 38.4$, (right) time history of the fluctuating magnetic field energy density.

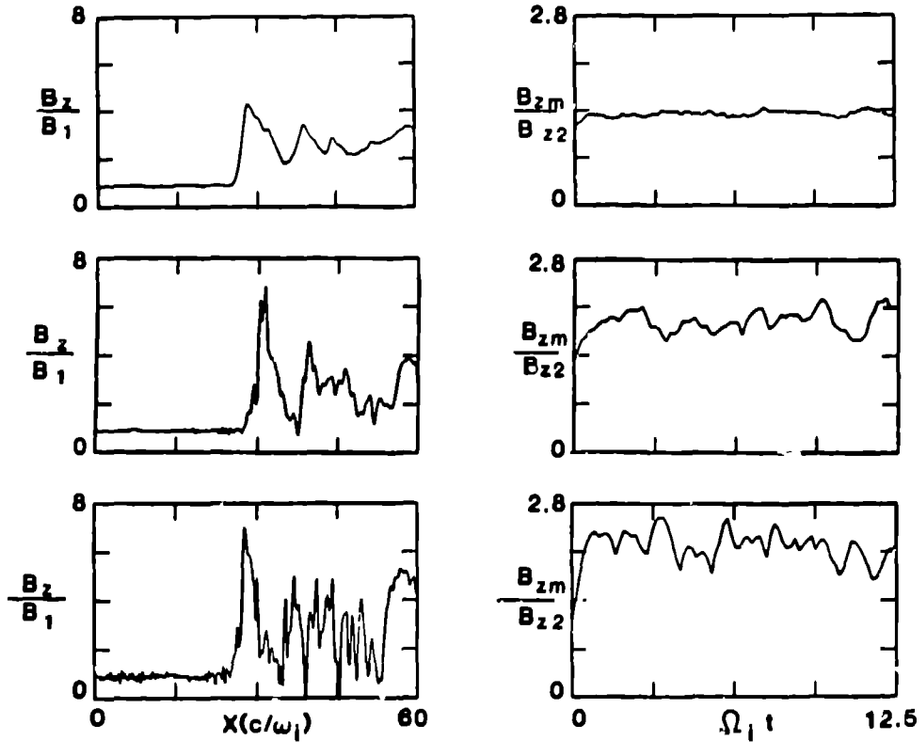

Figure 2. Results of three hybrid simulations for a quasiperpendicular shock (top: resistive code with large resistivity; middle: resistive code with smaller resistivity; bottom: predictor-corrector code) showing: (left) one component of the magnetic field at $\Omega_i t = 12.5$, (right) time history of the magnetic field overshoot.